VIRAL IMMUNOLOGY
Volume 13, Number 1, 2000
Mary Ann Liebert, Inc.
Pp. 93–106

Characterization of Protection Against Coronavirus Infection by Noninternal Image Antiidiotypic Antibody

MATHILDE W.N. YU and PIERRE J. TALBOT

ABSTRACT

Previously, we have reported protective vaccination of mice against a coronavirus infection using rabbit polyclonal noninternal image Ab2$_\gamma$ anti-idiotypic (anti-Id) antibody specific for a virus-neutralizing and protective monoclonal antibody (mAb) 7-10A against the viral surface S glycoprotein. To characterize further the mechanisms involved in the induction of protective immunity by this noninternal image anti-Id, plasma and splenocytes from Ab2$_\gamma$-immunized BALB/c mice were passively transferred to naive BALB/c mice, followed by viral challenge. A reproducible significant delay in mortality observed in mice to which plasma was passively transferred, together with the presence of specific *in vitro* neutralizing antiviral Ab3 identified the humoral immune response as the major element responsible for protection. The activation of specific and cross-reactive T lymphocytes by both virus and anti-Id in immunized mice and the absence of adoptive transfer of protection by splenocytes suggested the participation of T helper activity in the induction of protective virus-neutralizing Ab3. To obtain more defined monoclonal reagents for a better understanding of anti-Id-induced protection, mAb2 were generated against the same mAb1 7-10A and characterized. We report the successful generation of mAb2 of the γ type. However, unlike the polyclonal Ab2$_\gamma$, they were not capable of inducing a protective immune response.

INTRODUCTION

Murine hepatitis virus (MHV) is an enveloped RNA virus of the Coronaviridae family (14). Strain A59 of MHV (MHV-A59) is neutrotropic and causes an acute lethal encephalitis that is followed by chronic multiple sclerosis-like demyelination in mice that survive the acute disease (5,36). Among the major viral structural proteins, the surface (S) glycoprotein, which constitutes the spike projections, is responsible for important biological properties of the virus such as attachment to the cellular receptor and cellular membrane fusion (6,31). It is also a major target of the antiviral immune response: virus-neutralizing antibodies have been demonstrated to protect passively against acute infection (4,8,33–35), although cell-mediated immunity was also reported to be involved in protection (29,30,37).

We have been using the coronavirus animal model to characterize the immune modulation properties of the idiotypic network in the context of a viral infection. This network hypothesis of interactions between

Laboratory of Neuroimmunovirology, Human Health Research Center, INRS-Institut Armand-Frappier, Université du Québec, Laval, Québec, Canada H7V 1B7.

variable regions of immunoglobulins (17) has led to the concept that internal image anti-idiotypic antibody (anti-Id), which mimic the antigen (Ag), could be used as a surrogate Ag to induce a specific immune response, with some reported successes (3,12,32), including the activation of T lymphocytes (11). We and others have reported that noninternal image anti-Id could also induce protective immunity (22,39).

In a recent study, we showed that a rabbit polyclonal noninternal image anti-Id, identified as $Ab2_\gamma$ because the Ab2 preparation did not contain detectable internal image activity, induced a protective anti-MHV immune response in genetically different strains of mice (40). This anti-Id, produced by immunization with a virus-neutralizing and protective mAb specific for the viral S glycoprotein, induced specific antiviral antibodies in protected mice, although the importance of these antibodies in protection was not directly evaluated.

We now report studies designed to devaluate the mechanisms involved in protection induced by this noninternal image $Ab2_\gamma$ anti-Id. Monoclonal anti-Ids (mAb2) were also produced to obtain more defined monoclonal reagents for a better understanding of anti-Id-induced protection. Our results indicate that the neutralizing antiviral activity in plasma of protected animals was an important element for protection. No complementary biological activities, such as *in vitro* antibody-dependent cell-mediated cytolysis (ADCC) and antibody-dependent complement-mediated cytolysis (ADCMC), were detected in the plasma of $Ab2\gamma$-immunized mice. Even though a cellular immune response was not directly involved in protection, $Ab2\gamma$ primed mice to elicit an *in vitro* T-cell proliferative response following stimulation with virus and $Ab2_\gamma$, and we demonstrate T-cell cross-reactivity between viral and anti-Id antigens.

MATERIALS AND METHODS

Animals. Four- to 5-week-old MHV-seronegative female BALB/c mice were purchased from Charles River, St-Constant, Québec, Canada.

Antibodies. The production and characterization of a mouse hybridoma secreting neutralizing mAb 7-10A, which is specific for a discontinuous epitope on the S glycoprotein of MHV-A59, was previously described (8). This antibody was purified by standard Protein-A–Sepharose chromatography (25). The preparation and characterization of a polyclonal rabbit anti-Id against mAb 7-10A was described previously (22).

Virus, cells, and viral production. The A59 strain of MHV was initially obtained from the American Type Culture Collection (ATCC; Rockville, MD), plaque-purified twice, and passaged four times at a multiplicity of infection (MOI) of 0.01 on DBT cells as described previously (7). DBT astrocytoma cells induced as described previously (21) were a kind gift of Dr. Michael J. Buchmeier (The Scripps Research Institute, La Jolla, CA). N-11 mouse microglial cells, immortalized as described previously (24), were a kind gift of Drs. Yves Lombard and Jacques Borg (Université Louis Pasteur de Strasbourg, Illkirch, France).

Persistently infected N-11 cells were obtained by infecting the cells with MHV-A59 at a MOI of 0.9. After a 60-minute incubation period at 37°C with 5% (vol/vol) CO_2, the cells were washed twice with 10 mL of phosphate-buffered saline (PBS), and 10 mL of RPMI medium supplemented with 10% (vol/vol) fetal calf serum (FCS) were then added. The infected cells were incubated at 37°C with 5% (vol/vol) CO_2 for 2 days before being passaged. Cells were tested at each passage for production of infectious virus by plaque assay, as described previously (7). Virus production levels varied between 3×10^4 and 2×10^7 pfu/mL.

Passive protection assay. Two groups of 6 BALB/c mice each were injected intraperitoneally, 6 hours before viral challenge, with plasma in quantity equivalent to plasma from 1.2 mice previously immunized with either $Ab2_\gamma$ or normal rabbit immunoglobulins (NRIg). Two other groups of 6 mice were injected intravenously, 1 hour before viral challenge, with 10^8 splenocytes, prepared as described below, from mice previously immunized with $Ab2_\gamma$ or NRIg (22). Finally, two other groups of 3 mice each were injected with both plasma and splenocytes before viral challenge.

Viral challenge consisted of an intracerebral injection of 5×10^5 pfu (10 LD_{50}) of MHV-A59. This viral dose reproducibly yielded 100% mortality by 5 days after infection. Survival was evaluated and its significance was calculated using the log rank test (1).

Splenocytes used for adoptive transfer were prepared as follows. Spleens were collected from $Ab2_\gamma$- or NRIg-immunized BALB/c mice, 10 days after the last boost, and teased apart with tweezers. After filtra-

tion through a nylon net, splenocytes were centrifuged at 200 × *g* for 10 min and red blood cells were lysed with 6 mL of 0.16 M ammonium chloride (Anachemia Canada Inc., Montréal, Québec, Canada) and 10 mM HEPES (Canadian Life, Technologies, Inc., Burlington, Canada). After 10 minutes of incubation on ice, splenocytes were washed twice in RPMI medium supplemented with 2% (vol/vol) FCS and counted.

Antibody-dependent complement-mediated cytotoxicity. Approximately 1.5×10^7 N11 cells persistently infected with MHV-A59 were labeled with 600 μCi of sodium chromate ($Na_2{}^{51}CrO_4$, ICN Pharmaceuticals Canada Ltd., Montréal, Québec, Canada) for 18 hours at 37°C with 5% (vol/vol) CO_2. Labeled target cells were then washed four times with Hanks' balanced sodium salts (HBSS) (Canadian Life Technologies) and detached from the culture flask by adding 0.4 mM ethylene diamine tetracetic acid, tetrasodium salt (EDTA) (Anachemia Canada Inc.) and incubated for 5 minutes.

Target cells (10^4/well) were seeded into flat-bottomed 96-well plates and allowed to bind to the plastic for 2 hours at 37°C. The medium was then aspirated and serial three-fold dilutions of mouse plasma were added in triplicate to the target cells. After incubation for 1 hour at 37°C, the antibodies were aspirated, and 100 μL/well of rabbit complement (Pel-Freez, Rogers, AK) was added and allowed to react for 45 minutes at 37°C. For determination of spontaneous and maximum release, medium or 5% (vol/vol) Triton X-100 was added to the wells, respectively. After the incubation, 100 μL/well of RPMI without FCS was added. The cells were then centrifuged at 200 × *g* for 8 minutes, and 150 μL of supernatant was collected and counted for radioactivity in a Beckman Gamma 7000 counter (Beckman Instruments Canada Inc., Mississauga, Ontario, Canada). A mAb against ICAM-1 was used as a positive control mAb (YN1/1.7.4, CRL 1818; ATCC). It was a kind gift of Dr. Yves St-Pierre (INRS-Institut Armand-Frappier). Results are expressed as percent specific release:

$$100 \times (\text{cpm experimental} - \text{cpm spontaneous})/(\text{cpm maximum} - \text{cpm spontaneous})$$

Antibody-dependent cell-mediated cytotoxicity. Serial three-fold dilutions of decomplemented mouse plasma were diluted in quadruplicate in flat-bottomed 96-well plates for a final volume of 50 μL per well. Ten thousand target cells/well (50 μL), prepared as described above, were added to the diluted sera and the mixture was incubated for 1 hour at 37°C. One hundred microliters containing 10^6 splenocytes from BALB/c mouse were then added to each well containing the mixture of target cells and sera. Plates were centrifuged at 200 × *g* for 5 minutes. For determination of spontaneous and maximum release, medium or 5% (vol/vol) Triton X-100 were added to the wells, respectively. Plates were incubated for 6 hours at 37°C with 5% (vol/vol) CO_2. At the end of the incubation period, plates were centrifuged at 200 × *g* for 5 minutes, and 150 μL of supernatant was collected and counted for radioactivity and the results expressed as described above.

Ab2-induced cellular proliferation. Lymphocytes from immunized mice were obtained from inguinofemoral and axillary lymph nodes (draining the site of immunization), 10 days after two subcutaneous immunizations with either 100 μg of Ab2 or MHV-A59-infected cell lysates performed at 10-day intervals. Lymph nodes were dissociated, washed twice, and placed in 96-well flat-bottomed microtiter plates by adding 5×10^5 cells per well, along with various antigens. The specific and control antigens were 0.1 μg of concanavalin A (ConA), 10 μg of infected and noninfected cell lysate, 100 μL of supernatant of infected cells, and 10 μg of Ab2 or NRIg per well. Cultures were maintained at 37°C supplemented with 5% (vol/vol) CO_2 for 4 days. Eighteen hours before harvesting, 1 μCi of [^{3}H]thymidine (ICN Pharmaceuticals, Inc., Irvine, CA) was added to each well. Cells were harvested onto glass microfiber filter paper (Skatron Instruments Inc., Sterling, VA) on a 96-well Skatron model 11050 Micro cell harvester and counted in 5 mL of Ecolite (+) scintillation fluid (ICN), using a Canberra Packard Tri-Carb 2200A scintillation counter. Tests were run in triplicate. A stimulation index was calculated for each triplicate assay by dividing the mean radioactivity of stimulated cells by that of unstimulated cells. A value of at least 3.0 is considered significant.

Viral antigens used in these assays were prepared from DBT cells infected with MHV-A59 at an MOI of 1 at 37°C for 11 hours. Control antigens were prepared from parallel cultures of uninfected DBT cells. Infected and noninfected adherent cells were washed twice with 10 mL of PBS, pH 7.4, and frozen at −90°C overnight in 3 mL of PBS, pH 7.4. The cells were thawed at 37°C and detached from the plastic. The pooled

cells were sonicated (BraunSonic 2000) 2× 1 min with a 0.5-minute delay between the sonications, centrifugated at 500 × *g* for 10 minutes and stored in aliquots at −90°C. Before use, infectious virus in the viral preparation was inactivated by exposure to ultraviolet light (Ultraviolet illuminator, Model 3-3000, Fotodyne, New Berlin, WI, USA) for 10 minutes.

Virus neutralization assay. Serial three-fold dilutions of mouse plasma were incubated in tubes with approximately 80 plaque-forming units (pfu) of MHV-A59 for 60 minutes at 37°C. The mixtures were transferred in duplicate onto 12-well plates (ICN) containing confluent monolayers of DBT cells. After a 60-minute incubation at 37°C with 5% (vol/vol) CO_2, the virus–antibody mixtures were removed and the cells were overlaid with 1.5% (wt/vol) Bacto-Agar (Difco Laboratories, Detroit, MI) in Earle's minimal essential media/Hanks' M199 (1:1 (vol/vol) (Canadian Life Technologies Inc.) supplemented with 5% (vol/vol) FCS and 50 μg/mL gentamicin (Canadian Life Technologies, Inc.). The plates were incubated for 48 hours at 37°C with 5% (vol/vol) CO_2. The cells were then fixed with 25% (vol/vol) formalin and stained with 0.1% (wt/vol) crystal violet. Plaques were counted visually, and viral neutralization titers were expressed as the reciprocal of the plasma dilution that neutralized 50% of viral input. A known virus-neutralizing mAb was used as positive control.

Immunizations and cell fusions. Four BALB/c mice were immunized intraperitoneally with 100 μg of mAb 7-10A coupled to keyhole limpet hemocyanin (KLH) and emulsified in complete Freund's adjuvant (1:1, vol/vol) for the first injection. For the two subsequent booster doses, mice were immunized with 50 μg of mAb 7-10A using incomplete Freund's adjuvant (1:1, (vol/vol) at 12-week intervals. Three days before fusion, 100 μg of mAb 7-10A in PBS, pH 7.4, were injected intravenously. Mice were sacrificed, and spleen cells were fused with P3X63-AG8.653 nonsecreting mouse myeloma cells (ATCC) at a ratio of 5:1, using polyethylene glycol 1450 (Eastman Kodak Company, Rochester, NY). The fusion technique used was described previously (8), except that spleen macrophages were eliminated by adherence to a 150-mm plastic Petri dish (Canadian Life Technologies) in RPMI medium containing 10% (vo/vol) FCS, 1 mM sodium pyruvate, 2.5 mg/mL fungizone, 50 μg/mL gentamicin (Canadian Life Technologies, Inc.) for 1 hour at 37°C. The nonadherent cells were washed off with 10 mL of warm medium. After fusion, the culture medium was supplemented with 10% (vol/vol) of BM-Condimed® H1 hybridoma cloning supplement (Roche Diagnostics, Laval, Québec) and 50 nM of β-mercaptoethanol [Bio-Rad Laboratories (Canada) Ltd., Mississauga, Ontario].

Isotype determination. The immunoglobulin isotype was determined by a double immunodiffusion assay (2). Five milliliters of 1% (wt/vol) Seakem agarose gel (FMC Bioproducts, Rockland, ME) in PBS, pH 7.4, was melted and then solidified on 5-cm × 5-cm glass plates (thickness of approximately 2.5 mm). A central hole of 3-mm diameter was punched in the agarose gel surrounded by five other holes. Thirty microliters of mAb2 hybridoma supernatant were added in the central hole, and 10 μL of specific antiserum to IgG_1, IgG_{2a}, IgG_{2b}, IgG_3, IgA, and IgM (Cappel, Organon Teknika, West Chester, PA) in the other holes. Plates were incubated at 37°C for 18 hours until precipitation bands were visible.

ELISA for determination of mAb2 specificity. Ninety-six-well microtiter plates (ICN Pharmaceuticals Canada Ltd.) were coated with 60 ng/well of purified $F(ab')_2$ fragments of mAbs 7-10A and B35 (the latter used as an isotypic control) and KLH. The plates were incubated for 16 hours at room temperature. Then, the plates were blocked with 150 μL of PBS, pH 7.4, containing 10% (vol/vol) FCS and 0.2% (vol/vol) Tween-20 (ELISA blocking solution) for 30 minutes at 37°C. Serial five-fold dilutions of 15 μg/well of mAb2 in ELISA blocking solution were added to the wells and incubated for 90 min at room temperature. Wells were washed five times with PBS containing 0.1% (vol/vol) Tween-20 (PBS-T), and 100 μL of peroxidase-labeled anti-Fc fragment of mouse immunoglobulin conjugate (ICN ImmunoBiologicals, Costa Mesa, CA) diluted 1/2,000 was then added. Plates were then incubated for 90 minutes at room temperature. Plates were washed five times with PBS-T, and specific mAb binding was revealed by the addition of 100 μL of 2.2 mM *O*-phenylenediamine and 3 mM hydrogen peroxide. The enzymatic reaction was stopped with 100 μL of 1 N HCl, and the absorbance read at 492 nm using an SLT EAR 400 AT plate reader (SLT-Labinstruments, Austria).

ELISA for detection of inhibition of binding of Id to Ag by anti-Id and inhibition of virus-neutralization assay. This was performed as described previously (22).

Mab2 immunization and protection assay. Groups of 6 or 15 BALB/c mice were immunized by intraperitoneal injection of 100 μg of mAb2 coupled to KLH and emulsified in complete Fruend's adjuvant

(1:1, vol/vol) for the first injection. For the two subsequent booster doses, 50 μg of mAb2 emulsified in incomplete Freund's adjuvant (1:1, vol/vol) were given at 14-day internals. Seven days after the last injection, blood samples were drawn from the retroorbital plexus. An intracerebral viral challenge was given 3 days later with 10 LD_{50} (27) of MHV-A59 (equivalent of approximately 5×10^5 pfu).

RESULTS

Previously, we have reported that a polyclonal noninternal image anti-Id antibody induced antiviral antibodies that correlated with protection of mice from a normally lethal viral challenge (40). Data obtained with MHC-congenic mice supported the conclusion that both H-2- and non-H-2-dependent gene factors were involved in anti-coronavirus vaccination with $Ab2_\gamma$. To characterize further protective immune responses induced by this noninternal image anti-Id, we wanted to identify the major elements involved in antiviral protection and to determine whether mechanisms other than direct antibody-mediated virus neutralization were involved.

To characterize the possible involvement of humoral and/or cellular components in the protective immune response, plasma and/or splenocytes of immunized BALB/c mice were transferred to naive BALB/c mice before a normally lethal intracerebral challenge with 10 LD_{50} of MHV-A59. Results are shown in Fig. 1. Mice that received plasma, splenocytes, or both from mice immunized with NRIg died within 4 days after the viral challenge. However, a statistically significant and reproducible delay in mortality ($p < 0.001$) was observed with naive mice that received a passive transfer of serum from $Ab2_\gamma$-immunized mice. This significant 3-day delay in mortality suggests the important role played by plasma components in protection against infection by this coronavirus. A small and reproducible delay in mortality was also observed in mice

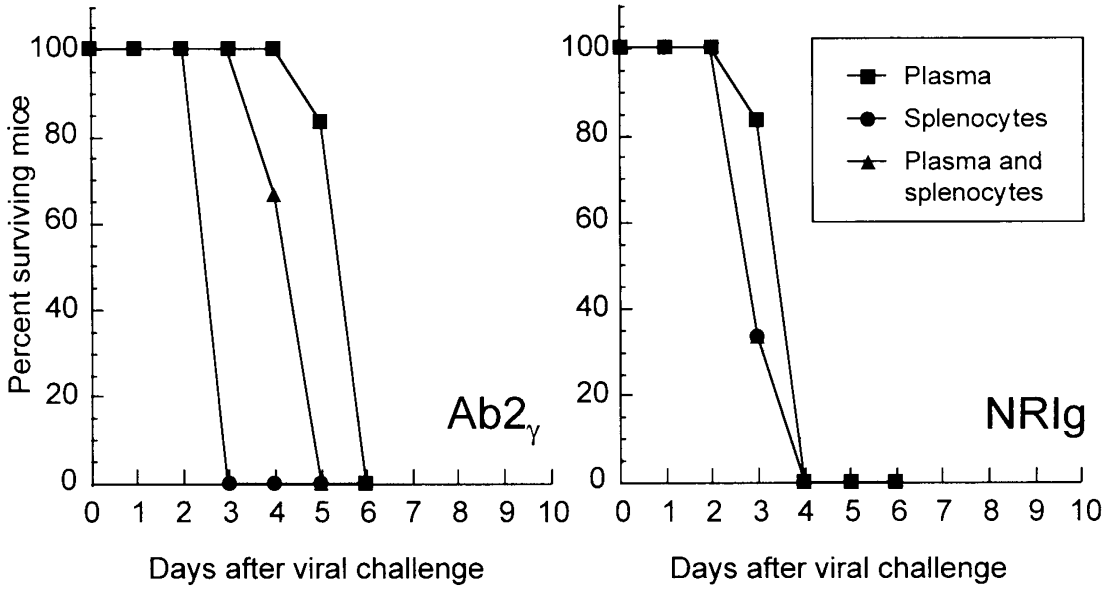

FIG. 1. Protection assay illustrating the involvement of plasma components in $Ab2_\gamma$-mediated vaccination of mice. In a first group of BALB/c mice, plasma from $Ab2_\gamma$- or NRIg-immunized mice was passively transferred to 6 naive BALB/c mice. In a second group of mice, splenocytes from $Ab2_\gamma$- or NRIg-immunized mice were adoptively transferred to 6 other naive mice. In a third group of mice, plasma and splenocytes from $Ab2_\gamma$- or NRIg-immunized mice were transferred together into 3 naive mice. Mice were then challenged with 10 LD_{50} of MHV-A59. The statistical significance of the delays in mortality were analyzed by the log rank test and only passive transfer of plasma was determined to be statistically significant ($p < 0.001$). The results presented are representative of two separate experiments, with very similar results.

that received a combination of plasma and lymphocytes, although statistical significance was not achieved. No difference in mortality was observed for mice that received an adoptive transfer of splenocytes from $Ab2_\gamma$-immunized BALB/c mice, suggesting that these cells were not directly involved in protection.

Immunization of mice with $Ab2_\gamma$ led to the production of virus-neutralizing Ab3. Virus neutralization activity was observed, with titers ranging between 100 and 3,000 in different strains of mice (22,40; data not shown). We also characterized antibody-mediated activities that may contribute to viral neutralization, such as ADCMC) and ADCC. These two biological activities were evaluated using N-11 target cells persistently infected with MHV-A59, without any observable virus-induced cytopathology. Plasma from $Ab2_\gamma$-protected BALB/c, DBA/1, DBA/2, and SWR mice (40) were tested. No ADCC or ADCMC activities were detected in $Ab2_\gamma$-immunized mice, using plasma dilutions as low as 1/50 for ADCC and 1/10 for ADCMC (data not shown). On the other hand, a control anti-ICAM-1 mAb in the ADCMC assay, showed 66% of lysed target cells in the presence of 5 μg of mAb (data not shown). Overall, these results suggest that the virus neutralization activity of Ab3 may be the major immune mechanism involved in $Ab2_\gamma$-induced protection.

Even though adoptive transfer studies suggested that splenocytes of $Ab2_\gamma$-immunized mice had no direct cytotoxic antiviral activity, we examined the participation of specific antiviral T lymphocytes in the observed Ab-mediated protection. To investigate the induction of specific cellular antiviral responses to polyclonal $Ab2_\gamma$, BALB/c mice were primed *in vivo* with $Ab2_\gamma$ or NRIg. Cells from lymph nodes of $Ab2_\gamma$-immunized BALB/c mice were used in an *in vitro* proliferation assay. These cells were stimulated *in vitro* with various concentrations of $Ab2_\gamma$, NRIg, virus, or with medium alone. As shown in Fig. 2, lymph node cells from $Ab2_\gamma$-immunized mice proliferated strongly in the presence of $Ab2_\gamma$, as expected, with a stimulation index of 29.5. Interestingly, these cells also proliferated in the presence of virus, with a significant stimulation index of 4.2. When lymph node cells of virus-immunized mice were stimulated with $Ab2_\gamma$, we observed significant proliferation, with a stimulation index of 6.7. As expected, these cells also proliferated strongly in the presence of virus. In this proliferation assay, virus supernatant showed a better stimulation capability than the infected cell lysate. This could be explained by toxicity generated from the cell lysate. This observed immune T-cell cross-reactivity suggests a role for T lymphocytes in the induction of specific neutralizing Ab3 by noninternal image $Ab2_\gamma$-immunized mice.

Previously, we have demonstrated the induction of a protective immune response against coronavirus infection with a polyclonal noninternal image $Ab2_\gamma$. This anti-Id was identified as an $Ab2_\gamma$ because no internal image activity was detected and it had the capacity to inhibit the binding of mAb1 7-10A to virus (22). However, the possible presence of traces of internal image anti-Id in the $Ab2_\gamma$ population that could be sufficient to induce the observed protection could not be excluded. Thus, more defined protective monoclonal anti-Id reagents need to be produced from the same mAb1 that induced the polyclonal $Ab2_\gamma$. Furthermore, the generation of monoclonal anti-Id antibodies (mAb2), would facilitate a more precise characterization of the protective immune response induced by noninternal image anti-Id.

Thus, four BALB/c mice were immunized with mAb1 7-10A coupled to KLH to generate mAb2. After four injections, mouse spleen cells were isolated and fused to myeloma cells. Hybridoma supernatant fluids were screened for the presence of anti-Id antibodies by ELISA using viral Ag as the coating Ag. The hybridoma in the positive wells was cloned and tested again for there specific reactivity to mAb1. Figure 3 illustrates that supernatant of hybridoma clones were specific to the idiotype of mAb1 because we observed a strong reactivity with mAb1 7-10A and only a background level response with another mAb (B35) of the same isotype. Also, mAb2 did not react with KLH, which was used as coupling molecule during immunization. As a positive control, the plasma of mice used for the cell fusion were also tested: it reacted with the idiotype, isotype and KLH as expected. (Fig. 3)

On the basis of the ability of Ab2 to inhibit the interaction between Ab1 and virus, $Ab2_\beta$ and $Ab2_\gamma$ can be differentiated from $Ab2_\alpha$: an $Ab2_\alpha$ is unable to inhibit Ab1 binding to Ag because it binds to idiotopes located away from the paratope of Ab1, whereas $Ab2_\beta$ and $Ab2_\gamma$ inhibit the interaction of Ab1 with virus by steric hindrance (γ) or by mimicry of the Ag (β). Thus, the hybridoma clones were examined further for inhibition of the binding of mAb1 7-10A to the virus. As illustrated in Fig. 4, mAbs secreted by some hybridoma clones showed more than 90% inhibition of binding of mAb1 to virus. Ten nanograms of mAb2 were enough to inhibit over 80% of mAb1 7-10A binding to virus, whereas the same amount of isotypic

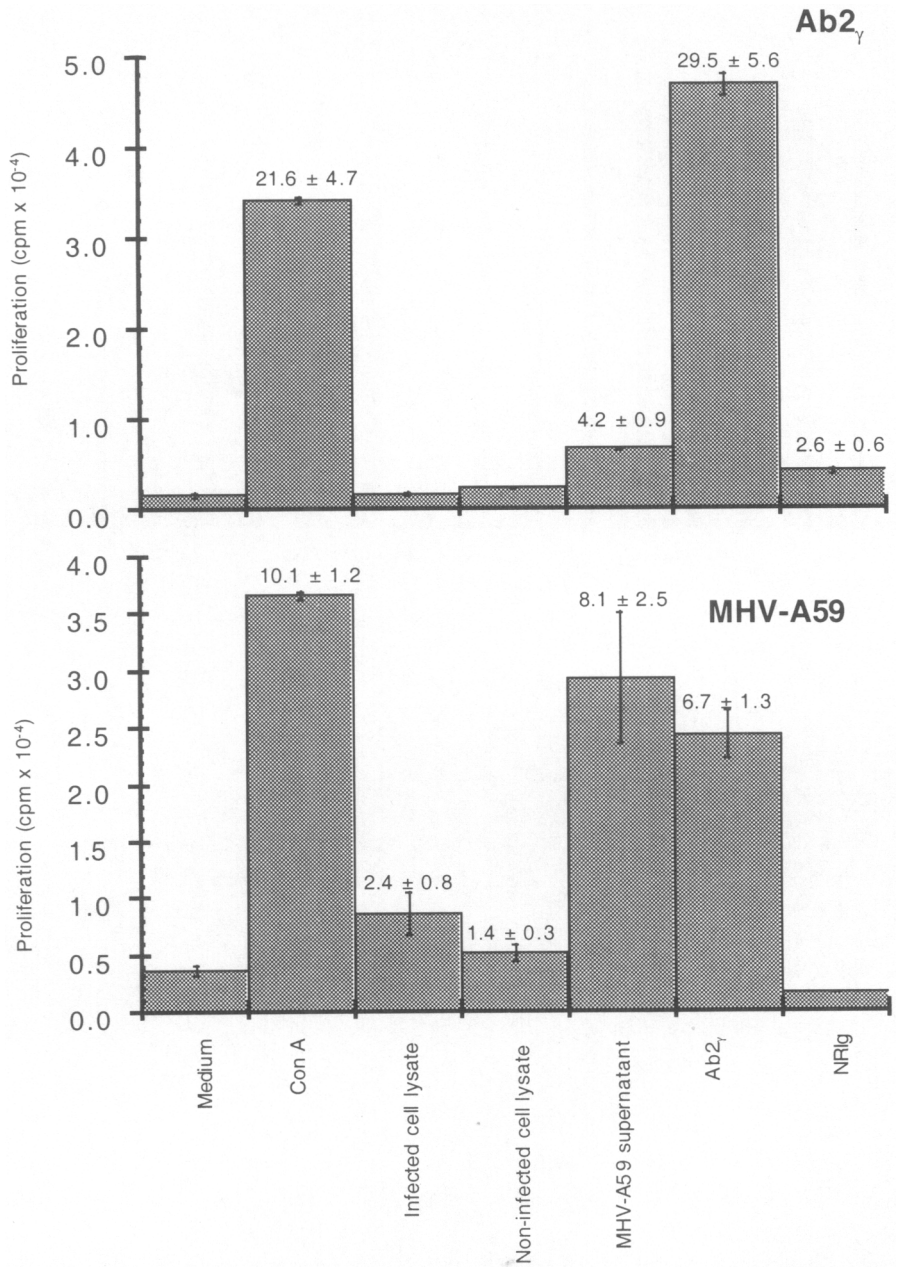

FIG. 2. Proliferation of lymph nodes cells from mice immunized with polyclonal $Ab2_\gamma$ (top panel) or MHV-A59 (bottom panel). Lymph node cells were stimulated *in vitro* with either 0.1 μg/well of ConA, 10 μg/well of infected or noninfected cell lysates, or 10 μg/well of $Ab2_\gamma$ or NRIg. Cells were harvested after 4 days of culture and the incorporation of [^{3}H]thymidine was quantitated. The stimulation indices were calculated for each triplicate by dividing the mean radioactivity of stimulated cells by that of unstimulated cells, and they are shown at the top of each box. The results presented are representative of two separate experiments, with very similar results.

control did not have any effect on this binding. However, mAbs secreted by other hybridoma clones inhibited binding of mAb1 to virus to a lesser extent. mAb2 were also tested for their capacity to inhibit virus neutralization by mAb1. Here again, the same clones exhibited inhibition confirming the inhibition of attachment assay. As shown in Table 1, a reduction of neutralization titers by 3 to 4 $\log_{10}$ was observed with as little as 10 μg of mAb2. Both results suggest that the sites recognized by mAb2 are located within or close to the antigen combining site of mAb1 and that these cells probably produce $Ab2_\beta$ or $Ab2_\gamma$. The other

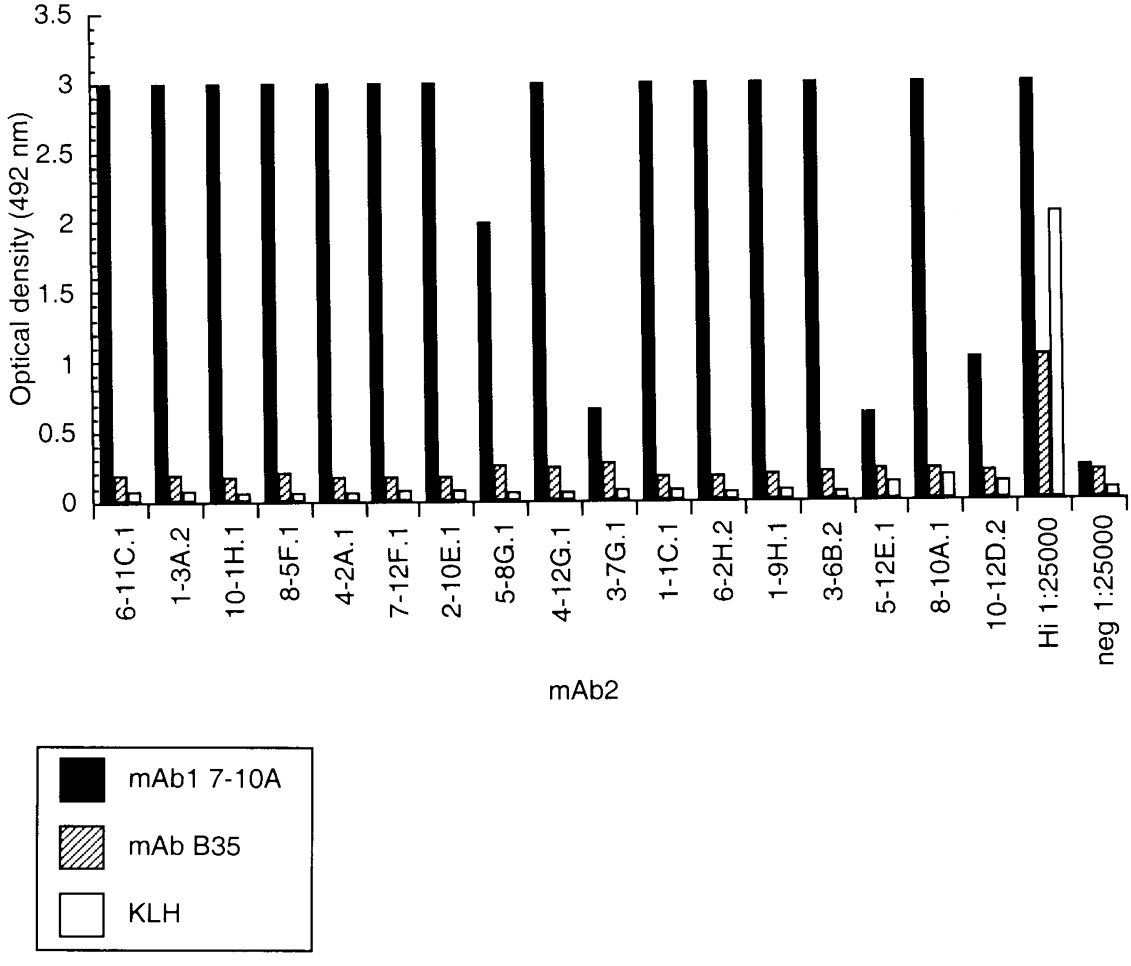

FIG. 3. ELISA for determining mAb2 specificity. Ninety-six-well microtiter plates were coated with 60 ng/well of $F(ab')_2$ fragments of mAb1, isotypic control mAb B35 (IgG_{2a}), or KLH, and binding of 4.8 ng/well of mAb2 supernatant or mAb 9E10.2 of the same isotype as the mAb2 (IgG_1) was determined using peroxidase-labeled mouse anti-Fc fragments. Hi, Hyperimmune plasma; neg, preimmune plasma.

mAb2 were identified as $mAb2_\alpha$. It is interesting to note that all the mAb2 generated in this experiment were of the IgG_1 isotype (Table 2).

The induction of Ag-specific immune response in animals immunized with anti-Id allows the distinction between internal image and noninternal image anti-Id. Moreover, in our goal to find protective mAb2, mice were immunized with mAb2 that were able to inhibit strongly the binding of mAb2 to virus and/or inhibit virus neutralization. After a first injection of 100 μg of mAb2 coupled to KLH and emulsified in Freund's adjuvant, and two booster injections of 50 μg, mouse plasma were tested for the presence of antiviral Ab3. None of the mAb2 induced detectable specific antiviral Ab3 by ELISA in immunized BALB/c mice (Table 2). However, because the polyclonal $Ab2_\gamma$ anti-7-10A had induced neutralizing Ab3 and the *in vitro* neutralization assay was more sensitive than ELISA, sera of mAb2-immunized mice were also tested for their capacity to neutralize viral infectivity. Again, no virus-neutralizing activity was detected with dilutions as little as 1/50 (Table 2). Ten days after the last booster immunization, mAb2-immunized mice were challenged intracerebrally with 10 LD_{50} of MHV-A59. None of the mAb2-immunized BALB/c mice survived the coronaviral challenge (Table 2). The absence of protection and the absence of induction of specific antiviral Ab3 in mAb2-immunized mice suggest that the mAb2 produced were not of the β-type, because structural mimicry would lead to the induction of specific antiviral Ab3.

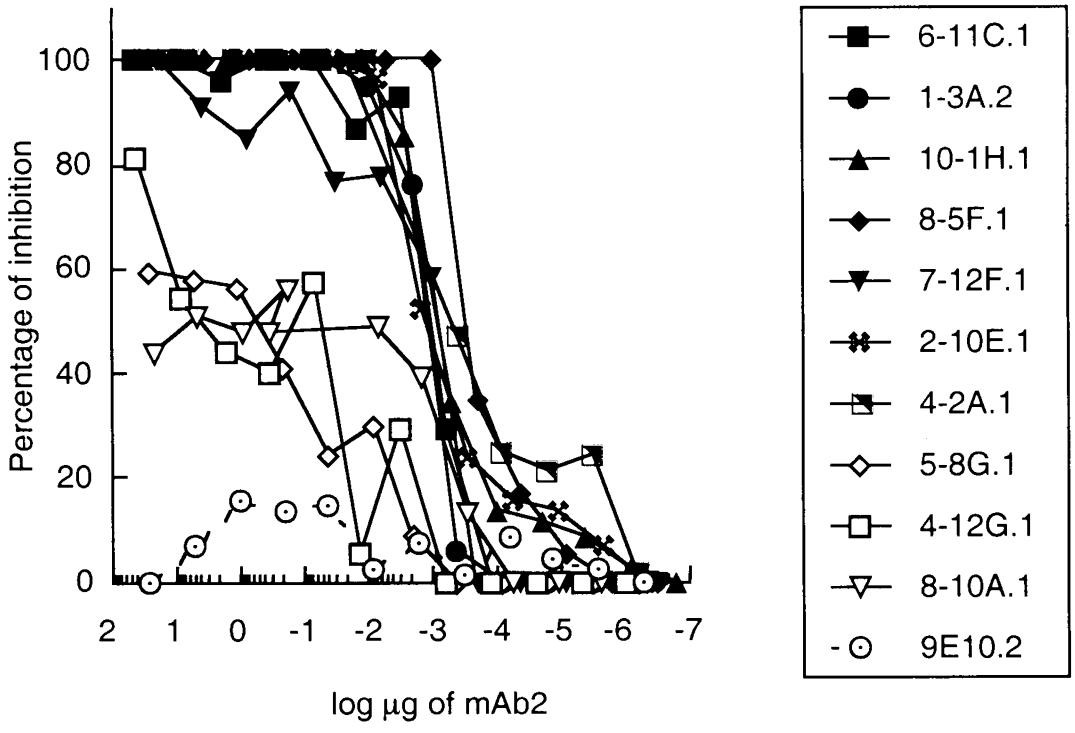

FIG. 4. Inhibition of binding of mAb1 to the virus by mAb2. Ninety-six-well microtiter plates were coated with 25 ng/well of viral Ag. Biotinylated mAb1 and dilutions of mAb2 supernatant or isotypic control mAb 9E10.2 were preincubated together and transferred onto the viral Ag-coated plates. The binding of mAb1 to viral Ag was detected using peroxidase-labeled streptavidin. The results of inhibition of binding of mAb1 to the virus by the isotypic control mAb 9E10.2 is represented by the dashed curve.

TABLE 1. INHIBITION OF MAB1 VIRUS NEUTRALIZATION WITH MAB2

mAb2 competitor	*Neutralization titer (log_{10})*[a]
6-11C.1	2
1-3A.2	3
10-1H.1	2
8-5F.1	2
7-12F.1	2
2-10E.1	3
4-2A.1	2
5-8G.1	6
4-12G.1	6
8-10A.1	6
9E10.2	6
Medium	6

[a]Reciprocal of the highest dilution of mAb1 7-10A ascites fluid that neutralized 50% of input virus after incubation with competitor mAb2.

TABLE 2. CHARACTERIZATION OF BIOLOGICAL PROPERTIES OF MAb2

MAb2	*Isotype*[a]	*Suggested nature of mAb2 type*	*Protection*	*Antiviral Ab3 (ELISA)*[b]	*Neutralizing antiviral Ab3*[c]
6-11C.1	IgG_1	γ	0/5	<1/100	<1/50
1-3A.2	IgG_1	γ	0/6	<1/100	<1/50
10-1H.1	IgG_1	γ	0/6	<1/100	<1/50
8-5F.1	IgG_1	γ	0/6	<1/100	<1/50
4-2A.1	IgG_1	γ	0/6	<1/100	<1/50
7-12F.1	IgG_1	γ	0/6	<1/100	<1/50
2-10E.1	IgG_1	γ	0/6	<1/25	ND[d]
5-8G.1	IgG_1	α	0/6	<1/25	ND
4-12G.1	IgG_1	α	0/6	<1/25	ND
3-7G.1	IgG_1	α	0/6	<1/25	ND
1-1C.1	IgG_1	γ	0/15	<1/25	ND
6-2H.2	IgG_1	α	0/6	<1/25	ND
1-9H.1	IgG_1	γ	0/6	<1/25	ND
3-6B.2	IgG_1	γ	0/6	<1/25	ND
5-12E.1	IgG_1	α	0/6	<1/25	ND
8-10A.1	IgG_1	α	ND	ND	ND
10-12D.2	IgG_1	α	0/6	<1/25	ND

[a]Immunoglobulin isotype determined by a double-immunodiffusion assay.
[b]Highest plasma dilution where specific antiviral Ab3 was detectable by ELISA.
[c]Plasma dilution that neutralized 50% of input virus.
[d]Not determined.

DISCUSSION

Previously, we have reported that a noninternal image polyclonal $Ab2_\gamma$ induced a specific antiviral protective immune response in different strains of mice and that this response was genetically controlled (22,40). In the present study, we provide evidence that is consistent with direct antibody-mediated neutralization representing the major protective immune response mechanism in vaccination by this noninternal image $Ab2_\gamma$. This is based on a reproducible and significant delay in mortality observed in naive BALB/c mice that received a passive transfer of plasma from $Ab2_\gamma$-immunized BALB/c mice, which contained *in vitro* neutralizing antibodies. Previously, we have shown that anti-Id immunization of BALB/c mice yielded complete protection of about 80% of animals (22,40). The fact that such a level of protection was not reproduced by passive plasma transfer may simply reflect the availability of lower quantities of protective antibodies in the target tissues.

Antiviral antibodies play an important role in the outcome of acute coronavirus disease in mice. Indeed, mAb against the S glycoprotein modulated MHV-JHM infection of mice from acute lethal encephalitis to chronic demyelinating disease (4). Moreover, neutralizing but also nonneutralizing specific antiviral mAb were shown to protect passively against lethal infection of mice (26). We previously demonstrated that mice immunized with affinity-purified S glycoprotein were protected from lethal encephalitis and developed high titers of neutralizing antibodies that correlated with protection (4).

Other antibody-mediated immune mechanisms were also reported to be activated upon infection of mice with coronaviruses. For example, C57BL/6 mice were shown to be high responders in the production of complement-fixing antibody compared to other strains of mice (26). However, the presence of these antibodies did not correlate with protection (26). Also, we have previously reported that peptide vaccination against acute murine coronavirus infection may be mediated by nonneutralizing antibodies (9). Thus, the antibody-dependent complement-mediated cytolysis and the antibody-dependent cell cytotoxicity were tested with the plasma of $Ab2_\gamma$-vaccinated BALB/c, DBA/1, DBA/2, and SWR mice. As we have reported

elsewhere, these strains of mice are protected against coronaviral infection by immunization with $Ab2_\gamma$ (40). No such Ab-mediated activities could be detected with the $Ab2_\gamma$-induced antiviral Ab3, which is consistent with direct antibody neutralization of viral infectivity. Unfortunately, we could not verify the presence of complement-fixing antibodies in C57BL/6 mice because they were not protected against the infection and did not produce detectable antiviral antibodies (40).

After adoptive transfer of splenocytes from $Ab2_\gamma$-immunized mice, no protection against lethal acute viral infection was observed, suggesting that the specific cellular immune response of $Ab2_\gamma$-immunized mice did not mediate direct antiviral cytotoxic activity. Cellular immune responses were reported to be important in protection against murine coronavirus infection: $CD4^+$ T cells with cytotoxic activity protected mice when adoptively transferred to naive mice (13,20,29). Furthermore, it was demonstrated that internal image anti-Id were able to induce an Ag-specific cellular immune response (10,32,38). In the current study, lymph node cells significantly proliferated in responses to viral Ag and $Ab2_\gamma$ (Fig. 2). This immune T-cell cross-reactivity suggests the participation of a cellular immune response of the helper type for T-dependent induction of antiviral antibodies by anti-Id.

In summary, plasma of $Ab2_\gamma$-immunized BALB/c mice contained the major immune component involved in the protective immune response against coronavirus infection. Furthermore, the major humoral mechanism used was most likely the virus neutralization activity of specific antiviral Ab3 induced with the collaboration of a helper T-cell-mediated immune response. Thus, our results are consistent with a T-dependent production of neutralizing and protective antiviral antibodies after immunization of some strains of mice with a noninternal image anti-Id.

Because mAb1 7-10A was able to produce a protective polyclonal $Ab2_\gamma$ in rabbits that induced neutralizing antiviral Ab3 when used as immunogen, mAb2 were generated to define more precisely the mechanism of protection of a homogenous population of anti-Id. We were able to select mAb2 that were specific to mAb1 7-10A. They were characterized as mAb2α or mAb2γ. All mAb2 were of the IgG_1 isotype, which corroborates another study that suggested that IgG_1 is the main isotype expressed in anti-idiotypic responses to idiotypes in mice and rat (27). Another study demonstrated that an anti-idiotypic antibody response is dependent on T-helper cells (16) and that thymus-dependent antigens predominantly stimulate IgG_1 in the mouse. Furthermore, Freund's adjuvant was reported to favor the production of antibodies of the IgG_1 isotype (18). Among all specific mAb2 isolated, six $mAb2_\gamma$ were selected for evaluation of potential protective activities. In contrast to the polyclonal $Ab2_\gamma$ generated from mAb1 7-10A-immunized rabbit, no mAb2γ-immunized BALB/c mice were protected against the lethal coronavirus infection or showed the induction of coronavirus-specific Ab3.

Results from a previous study (23) and the current study indicate that, in the MHV model, the production of protective mAb2 is technically difficult by the classical hybridoma technique (39). In another study using molecular biological technology, Ab2 clones were successfully selected using phage-displayed recombinant anti-idiotypic antibody scFv fragments library against coronavirus-neutralizing mAb. However, the selected anti-Id were not able to induce a protective immune response in mice (23). The results from these studies suggest the presence of a low frequency of protective anti-Id in the antibody repertoire. However, even the presence of low quantities of anti-idiotypic antibody seems to play an important role in the induction of the protection as shown with the protective polyclonal $Ab2_\gamma$.

Since no protective mAb2 were induced by mAb1 7-10A, in contrast to the protective polyclonal $Ab2_\gamma$ generated from this same mAb1, the possibility that there were traces of beta-type anti-Id, not detectable in the polyclonal $Ab2_\gamma$ population, could not be ruled out. However, the mAb2 were produced in a different animal species than the polyclonal $Ab2_\gamma$, and they may not necessarily share the same antibody repertoire. Indeed, the antibodies that recognize the idiotope of mAb1 responsible for the protection observed could be present in the rabbit and absent in the mouse. Furthermore, there are reports of induction of antigen-specific responses with monoclonal or polyclonal noninternal image anti-idiotypes (15,28,41), which is consistent with the antiviral immune response induced by our noninternal image $Ab2_\gamma$.

It is probable that the complexities of the idiotypic network will take time before being completely understood. This emphasizes the need to characterize further the mechanisms of protective immune response with anti-idiotypic antibodies before being able to manipulate the idiotypic network safely.

ACKNOWLEDGMENTS

This work was supported by grant MT-9203 from the Medical Research Council of Canada to P.J.T. and a studentship from the Fonds pour la formation et l'aide à la recherche due Québec to M.W.N.Y. A senior scholarship award from the Fonds de la recherche en santé du Québec to P.J.T. is gratefully acknowledged. We thank Francine Lambert for technical assistance and Tina Concetta Miletti for performing some of the experiments described in Table 2.

REFERENCES

1. Armitage, P., and G. Berry. 1987. Statistical methods in medical research. 2nd ed. Blackwell Scientific Publications, Oxford; pp. 428–433.
2. Bailey, G.S. 1984. Immunodiffusion in gels. In Walker, J.M. (ed): Methods in molecular biology. Proteins. Humana Press, Clifton, NJ; pp. 301.
3. Billetta, R., M.R. Hollingdale, and M. Zanetti. 1991. Immunogenicity of an engineered internal image antibody. Proc. Natl. Acad. Sci. USA 88:4713–4717.
4. Buchmeier, M.J., H.A. Lewicki, P.J. Talbot, and R.L. Knobler. 1984. Murine hepatitis virus-4 (strain JHM) induced neurologic disease is modulated in vivo by monoclonal antibody. Virology 132:261–270.
5. Cheever, F.S., J.B. Daniels, A.M. Pappenheimer, and O.T. Bailey. 1949. A murine virus (JHM) causing disseminated encephalomyelitis with extensive destruction of myelin. I. Isolation and biological properties of the virus. J. Exp. Med. 90:181–194.
6. Collins, A.R., R.L. Knobler, H. Powell, and M.J. Buchmeier. 1982. Monoclonal antibodies to murine hepatitis virus-4 (strain JHM) define the viral glycoprotein responsible for attachment and cell-cell fusion. Virology 199:358–371.
7. Daniel, C., and P.J. Talbot. 1987. Physico-chemical properties of murine hepatitis virus, strain A-59. Arch. Virol. 96:241–248.
8. Daniel, C., and P.J. Talbot. 1990. Protection from lethal coronavirus infection by affinity-purified spike glycoprotein of murine hepatitis virus, strain A59. Virology 174:87–94.
9. Daniel, C., M. Lacroix, and P.J. Talbot. 1994. Mapping of linear antigenic sites on the S glycoprotein of a neurotropic murine coronavirus with synthetic peptides: a combination of nine prediction algorithms fails to identify relevant epitopes and peptide immunogenicity is drastically influenced by the nature of the protein carrier. Virology 202:540–549.
10. Durrant, L.G., M. Doran, E.B. Austin, and R.A. Robins. 1995. Induction of cellular immune responses by a murine monoclonal anti-idiotypic antibody recognizing the 791Tgp72 antigen expressed on colorectal, gastric and ovarian human tumours. Int. J. Cancer 6:62–66.
11. Fagerberg, J., M. Steinitz, H. Wigzell, P. Askelöf, and H. Mellstedt. 1995. Human anti-idiotypic antibodies induced a humoral and cellular immune response against a colorectal carcinoma-associated antigen in patients. Proc. Natl. Acad. Sci. USA 92:4773–4777.
12. Fung, M.S.C., C.R.Y. Sun, R.S. Liou, W. Gordon, N.T. Chang, S.-W. Chang, and N.-C. Sun. 1990. Monoclonal anti-idiotypic antibody mimicking the principal neutralization site in HIV-1 GP120 induces HIV-1 neutralizing antibodies in rabbits. J. Immunol. 145:2199–2206.
13. Heemskerk, M.H.M., H.M. Schoemaker, W.J.M. Spaan, and C.J.P. Boog. 1995. Predominance of MHC class II-restricted $CD4^+$ cytotoxic T cells against mouse hepatitis virus A59. Immunology 84:521–527.
14. Holmes, K.V., and M.M.C. Lai. 1996. Coronaviridae: the viruses and their replication. In Fields, B.N., D.M. Knipe, P.M. Howley et al. (eds): Fields virology, 3rd ed. Lippincott-Raven Publishers, Philadelphia; pp. 1075–1093.
15. Huang, J.H., R.E. Ward, and H. Kohler. 1986. Idiotope antigens (Ab2 alpha and Ab2 beta) can induce in vitro B cell proliferation and antibody production. J. Immunol. 137:770–776.

16. Janeway, C.A. Jr., H.S. Koren, and P. We. 1975. The role of thymus-derived lymphocytes in an antibody-mediated hapten-specific helper effect. Eur. J. Immunol. 5:17–22.

17. Jerne, N.K. 1974. Towards a network theory of the immune system. Ann. Immunol. 125C:373–389.

18. Karagouni, E.E., and L. Hadjipetrou-Kourounakis. 1990. Regulation of isotype immunoglobulin production by adjuvants in vivo. Scand. J. Immunol. 31:745–754.

19. Köhler, G., and C. Milstein. 1975. Continuous cultures of fused cells secreting antibody of predefined specificity. Nature 256:495–497.

20. Körner, H., A. Schliephake, J. Winter, F. Zimprich, H. Lassmann, J. Sedgwick, S. Siddell, and H. Wege. 1991. Nucleocapsid or spike protein-specific $CD4^+$ T lymphocytes protect against coronavirus-induced encephalomyelitis in the absence of $CD8^+$ T cells. J. Immunol. 147:2317–2323.

21. Kumanishi, T. 1967. Brain tumors induced with Rous Sarcoma virus, Schmidt-Ruppin strain. I. Induction of brain tumors in adult mice with Rous chicken sarcoma cells. Jap. J. Exp. Med. 37:461–474.

22. Lamarre, A., J. Lecomte, and P.J. Talbot. 1991. Antiidiotypic vaccination against murine coronavirus infection. J. Immunol. 147:4256–4262.

23. Lamarre, A. and P.J. Talbot. 1998. Characterization of phage-displayed recombinant anti-idiotypic antibody fragments against coronavirus-neutralizing monoclonal antibodies. Viral Immunol. 10:175–181.

24. Lutz, M.B., F. Granucci, C. Winzler, G. Marconi, P. Paglia, M. Foti, C.U. Abmann, L. Cairns, M. Rescigno, and P. Ricciardi-Castagnoli. 1994. Retroviral immortalization of phagocytic and dendritic cell clones as a tool to investigate functional heterogeneity. J. Immunol. Methods 174:269–279.

25. Manil, I., P. Motté, P. Pernas, F. Troalen, C. Bohuon, and D. Bellet. 1986. Evaluation of protocols for purification of mouse monoclonal antibodies. J. Immunol. Methods 90:25–37.

26. Nakanaga, K., K. Yamanouchi, and K. Fujiwara. 1986. Protective effect of monoclonal antibodies on lethal mouse hepatitis virus infection in mice. J. Virol. 59:168–171.

27. Rousseaux-Prévost R., J. Bonneterre, H. Bazin, and J. Rousseaux. 1983. Subclass restriction of the antiiodiotypic antibody response in the rat. Ann. Immunol. (Inst. Pasteur) 134D:167–179.

28. Schick M.R., G.R. Dreesman, and R.C. Kennedy. 1987. Induction of an anti-hepatitis B surface antigen response in mice by noninternal image ($Ab2_\alpha$) anti-idiotypic antibodies. J. Immunol. 138:3419–3425.

29. Stohlman, S.A., G.K. Matsushima, N. Casteel, and L.P. Weiner. 1986. In vivo effects of coronavirus-specific T cell clones: DTH inducer cells prevent a lethal infection but do not inhibit virus replication. J. Immunol. 136:3052–3056.

30. Stohlman, S.A., C.C. Bergmann, R.C. van der Veen, and D.R. Hinton. 1995. Mouse hepatitis virus-specific cytotoxic T lymphocytes protect from lethal infection without eliminating virus from the central nervous system. J. Virol. 69:684–694.

31. Sturman, L.S., C.S. Ricard, and K.V. Holmes. 1985. Proteolytic cleavage of the E2 glycoprotein of murine coronavirus: activation of cell-fusing activity of virions by trypsin and separation of two different 90 K cleavage fragments. J. Virol. 56:904–911.

32. Su S., M.M. Ward, M.A. Apicella, and R.E. Ward. 1992. A nontoxic, idiotope vaccine against gram-negative bacterial infections. J. Immunol. 148:234–238.

33. Talbot, P.J., A.A. Salmi, R.L. Knobler, and M.J. Buchmeier. 1984. Topographical mapping of epitopes on the glycoproteins of murine hepatitis virus-4 (strain JHM): Correlation with biological activities. Virology 132:250–260.

34. Talbot, P.J., G. Dionne, and M. Lacroix (1988) Vaccination against lethal coronavirus-induced encephalitis with a synthetic decapeptide homologous to a domain in the predicted peplomer stalk. J. Virol. 62:3032–3036.

35. Wege, H., R. Dörries, and H. Wege. 1984. Hybridoma antibodies to the murine coronavirus JHM: Characterization of epitopes on the peplomer protein (E2). J. Gen. Virol. 65:1931–1942.

36. Weiner, L.P. 1973. Pathogenesis of demyelination induced by mouse hepatitis virus (JHM virus). Arch. Neurol. 28:298–303.

37. Yamaguchi, K., N. Goto, S. Kyuwa, M. Hayami, and Y. Toyoda. 1991. Protection of mice from a lethal coronavirus infection in the central nervous system by adoptive transfer of virus-specific T cell clones. J. Neuroimmunol. 32:1–9.

38. Yang, Y.-F., and Y. Thanavala. 1995. A comparison of the antibody and T cell response elicited by internal image and noninternal image anti-idiotypes. Clin. Immunol. Immunopathol. 75:154–158.

39. Yu, M., and P.J. Talbot. 1995. Induction of a protective immune response to murine coronavirus with non-internal image anti-idiotypic antibodies. Adv. Exp. Med. Biol. 380:165–172.

40. Yu, M.W.N., S. Lemieux, and P.J. Talbot. 1996. Genetic control of anti-idiotypic vaccination against coronavirus infection. Eur. J. Immunol. 26:3230–3233.

41. Zhou, E.-M., K.L. Lohman, and R.C. Kennedy. 1990. Administration of noninternal image monoclonal anti-idiotypic antibodies induces idiotype-restricted responses specific for human immunodeficiency virus envelope glycoprotein epitopes. Virology 174:9–17.

Address reprint requests to:
Dr. Pierre J. Talbot
Laboratory of Neuroimmunovirology
Human Health Research Center
INRS-Institute Armand-Frappier
Université du Québec
531 Boulevard des Prairies
Laval, Québec, Canada H7V 1B7

E-mail: Pierre.Talbot@inrs-iaf.uquebec.ca

Received for publication May 20, 1999; accepted September 23, 1999.